Electronic Supplementary Material (ESI) for Catalysis Science & Technology.
This journal is © The Royal Society of Chemistry 2018

Supplementary information

Supported gold-nickel nano-alloy as highly efficient catalyst in levulinic acid hydrogenation with formic acid as an internal hydrogen source

Agnieszka M. Ruppert,[a]* Marcin Jędrzejczyk,[a] Natalia Potrzebowska,[a] Kamila Kaźmierczak,[a] Magdalena Brzezińska,[a] Olga Sneka-Płatek,[a] Philippe Sautet,[b,d,e] Nicolas Keller,[c] Carine Michel,[b]* Jacek Grams[a]

[a.] *Institute of General and Ecological Chemistry, Faculty of Chemistry, Łódź University of Technology, ul. Żeromskiego 116, 90-924 Łódź, Poland. * E-mail: agnieszka.ruppert@p.lodz.pl; Fax: +48426313128; Tel: +48426313106*

[b.] *Univ Lyon, Ens de Lyon, CNRS UMR 5182, Université Claude Bernard Lyon 1, Laboratoire de Chimie, F69342, Lyon, France. * E-mail: carine.michel@ens-lyon.fr; Fax: +33472728080; Tel: +33472728847*

[c.] *Institut de Chimie et Procédés pour l'Energie, l'Environnement et la Santé, ICPEES, CNRS, University of Strasbourg, 25 rue Becquerel, 67087, Strasbourg, France.*

[d.] *Department of Chemical and Biomolecular Engineering, University of California, Los Angeles, Los Angeles, CA 90095, United States*

[e.] *Department of Chemistry and Biochemistry, University of California, Los Angeles, Los Angeles, CA 90095, United States*

Electronic Supplementary Information (ESI) :

Description of the preparation method of the monometallic catalysts ; details of the characterization techniques ; Figure S1 that represents the energy profiles for the formic acid decomposition through the carboxylate pathway on Au(111), Ni(111) and Au-Ni(111) ; Figure S2 and Figure S3 represent the computed structures of the intermediates and transition states on Au-Ni(111) ; Figure S4 represents the computed Gibbs energy profiles for Au (dotted), Ni (plain), Au-Ni bimetallic surfaces (dashed) with HCOOH dehydration *via* COOH. Figure S5 shows the XPS spectra recorded on the Au-$Ni_{(Cl)}$/γ-$Al_2O_{3(C)}$ catalyst ; Table S1 shows the catalytic activity of selected catalysts together with the selectivity towards gaseous products ; Table S2 shows the activity of Au-$Ni_{(Cl)}$/γ-$Al_2O_{3(C)}$ catalyst after recycling processes in the LA hydrogenation with FA as internal hydrogen source (FALA) ; Table S3 shows the normalized intensity of selected ions collected from the catalyst surface during ToF-SIMS analysis.

Experimental part

Preparation of the catalyst

The Au monometallic catalysts supported on γ-Al_2O_3 were prepared with a 1 wt.% metal content using aqueous solution of $HAuCl_4 \cdot 4H_2O$ (POCH S.A., pure) with a concentration of 4599.7 mg/L. The support was impregnated by chloroauric acid solution under reflux at 80°C, before urea was added dropwise as precipitating agent to achieve a concentration of 0.42 mol/L. Then the mixtures were cooled down.

In a first approach, the Au catalyst was first vacuum filtrated and dried at 120°C for 2 h. Then, the catalyst was calcined in 300°C for 4 h in air flow (20 mL/min) with heating rate of 10°C/min, and further reduced in hydrogen flow (60 mL/min) at 300°C for 1 h with a heating rate of 2°C/min. This sample is labeled as 1%Au/γ-$Al_2O_{3(C)}$.

In a second approach, the Au catalyst was reduced via the addition of a 5-times excess of sodium borohydrate ($NaBH_4$, Sigma Aldrich, 99%) for 15 min. Then the suspension was vacuum filtrated, washed with distilled water (500 mL) and finally dried at 80°C for 12 h. This sample is labeled as 1%$Au_{(CR)}$/γ-Al_2O_3.

The Ni monometallic catalysts supported on γ-Al_2O_3 were prepared with a 4 wt.% metal content using aqueous solution of $Ni(NO_3)_3 \cdot 6H_2O$ (Chempur, pure) with a concentration of 8420 mg/L. The support was impregnated by the metallic salt solution.

In a first approach, the Ni catalyst suspension was first aged for 24 h at room temperature. After evaporation of water, it was dried at 120°C for 2 h. The Ni catalyst was then calcined in air at 500°C for 5 h (heating rate of 5°C/min) and further reduced in hydrogen flow (60 mL/min) at 550°C for 1 h with a heating rate of 10°C/min. This sample is labeled as 4%Ni/γ-$Al_2O_{3(C)}$.

In a second approach, the Ni catalyst was reduced via the addition of a 5-times excess of $NaBH_4$ for 15 min. Then the suspension was vacuum filtrated, washed with distilled water (500 mL) and finally dried at 80°C for 12h. This sample is labeled as 4%$Ni_{(CR)}$/γ-Al_2O_3.

The Ru monometallic catalysts supported on TiO_2 P25 and ZrO_2 were prepared with a 5 wt.% metal content using aqueous solution of $RuCl_3$ (Merck Millipore) with a concentration of 177 mg/L. Zirconia support was obtained by calcining $ZrO(NO_3)_3{\cdot}6H_2O$ (Sigma-Aldrich) at 500°C for 4 h in air with a heating rate of 10°C/min. The supports were impregnated by the solution of $RuCl_3$ and aged for 24 h at room temperature. After evaporation of water, the catalysts were dried at 120°C for 2 h and reduced in hydrogen flow at 500°C for 1h with a heating rate of 10°C/min. Those samples are labeled as 5%Ru/TiO_2 and 5%Ru/ZrO_2, respectively.

Characterization techniques

Secondary ion mass spectra were recorded with a time-of-flight secondary ion mass spectrometer (ToF-SIMS IV) manufactured by ION-TOF GmbH, Germany. Bi_3^+ was used as a primary ion source. The measurements were performed in the static mode. The samples were fixed to the sample holder by double sided adhesive tape. The analyzed area of the sample surface was 500 µm × 500 µm. During analysis, a pulsed low-energy electron flood gun was used for charge neutralization. The experiments were repeated three times for each sample.

X-ray diffraction (XRD) measurements were collected using a PANalytical X'Pert Pro MPD diffractometer. The X-ray source was a copper long fine focus X-ray diffraction tube operating at 40 kV and 30 mA. Data were collected in the 5–90° 2Θ range with 0.0167o step. Crystalline phases were identified by references to ICDD PDF-2 (version 2004) database. All calculations were performed with X'Pert High Score Plus computer program.

The surface area and porosimetry measurements were carried out on automatic sorptometer Micromeritics ASAP 2020 V3.05 G (Surface Area and Porosity Analyzer). Samples were outgassed at 300°C during 4 hours evacuation and after that low temperature nitrogen adsorption-desorption measurements were carried out using BET, liquid N_2 method. The BET specific surface area was calculated from the N_2 adsorption isotherm.

Transmission electron microscopy (TEM) and energy dispersive X-ray (EDX) measurements were carried out using JEM 2010 microscope at an accelerating voltage of 200 kV with LaB_6 emission current. Samples were suspended in ethanol and deposited onto carbon-coated copper grids before examination. For each catalyst, from 400 to 700 individual Au-Ni particles were counted. The average crystallite diameter (d) was calculated from the formula:

$$d = \frac{\sum_i n_i d_i^3}{\sum_i n_i d_i^2}$$

where n_i is the number of particles of diameter d_i.

Scanning transmission electron microscopy (STEM) observations were conducted using a JEM-2100F (FEG, 200 kV) equipped with a probe aberration corrector, a high-angle annular dark field (HAADF) detector, and EDX spectrometer. For STEM investigations, the dry samples were crushed in air using glass slides and were casted on copper TEM grids covered with holey carbon.

Temperature-programmed reduction (TPR) was performed on AMI1 system from Altamira Instruments, USA, equipped with a thermal conductivity detector and was used for examining the reducibility of catalysts. The monometallic and bimetallic Au-Ni catalysts were calcined at 200°C (with heating rate of 10°C/min) for 30 min in a mixture of 2 vol.% O_2 and 98 vol.% Ar at space velocity W/F = 1.11×10^{-5}g/h cm^3, before the TPR measurements. The mixture of 5 vol.% H_2 and 95 vol.% Ar with the same space velocity as above was used. TPR profiles were recorded from 30°C up to 600°C, with a heating rate of 10°C/min.

X-Ray Photoelectron Spectroscopy (XPS) surface characterisation was performed using an Axis Ultra^{DLD} spectrometer (Kratos Analytical) equipped with a Al K_α (1486.6 eV) monochromatic source (pass energy of 40 eV). The spectra were decomposed assuming contributions with a Doniach-Sunjic shape[1] and a Shirley background subtraction.[2] The Al 2p band at 74.6 eV was used as the binding energy reference to compensate for energy shifts due to electrostatic charging. The apparatus is equipped with a thermal treatment chamber operating under controlled atmosphere.

Analysis of the gaseous reaction products

The gaseous products were analyzed by gas chromatography (VEB Chromatrom, Berlin) equipped with a TCD detector. Argon was used as the carrier gas with a flow rate of 15 ml min−1 and the injections were performed with a volume of 2 ml.

Results

Theoretical study

Figure S1 represents the energetic profiles for the HCOOH decomposition pathways via COOH intermediate for monometallic (Au (111), Ni (111)) and bimetallic (Au-Ni (111)) surfaces. On Figure S2 and S3 are presented the images for molecules and intermediates among the two decomposition pathways: *via* HCOO and *via* COOH, respectively.

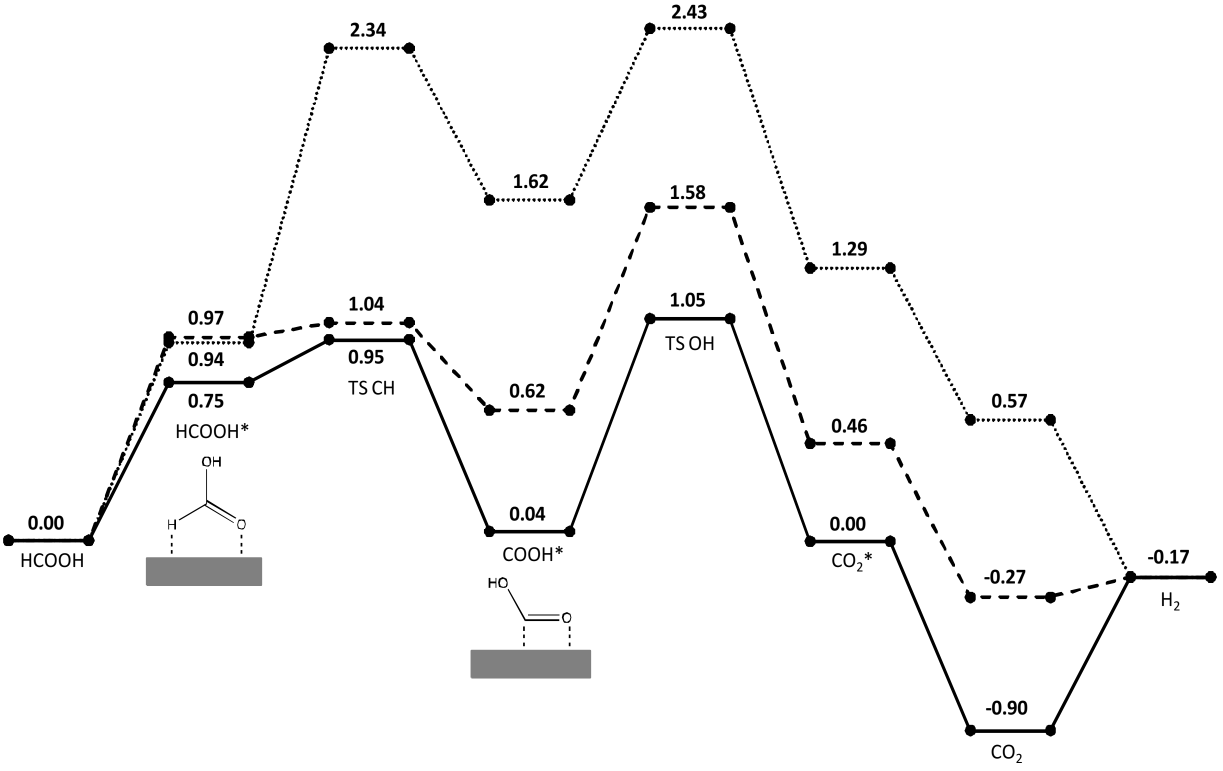

Figure S1. HCOOH dehydrogenation *via* COOH. Gibbs energy profiles for Au (dotted), Ni (plain), Au-Ni bimetallic surfaces (dashed). Gibbs energies given in eV at T=190°C; * means adsorption at the surface.

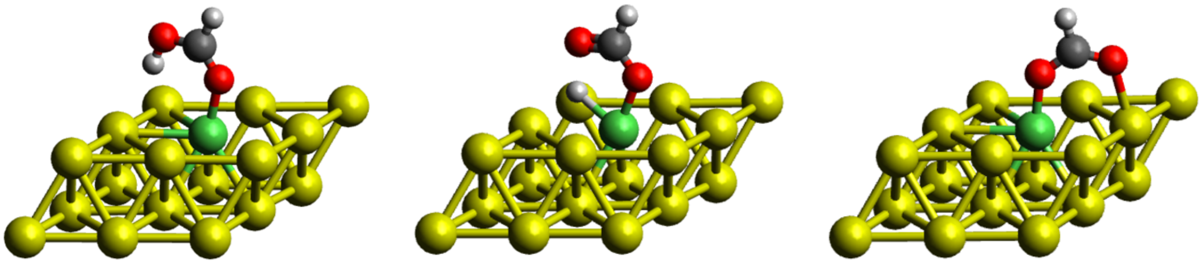

HCOOH TS OH HCOO$_B$

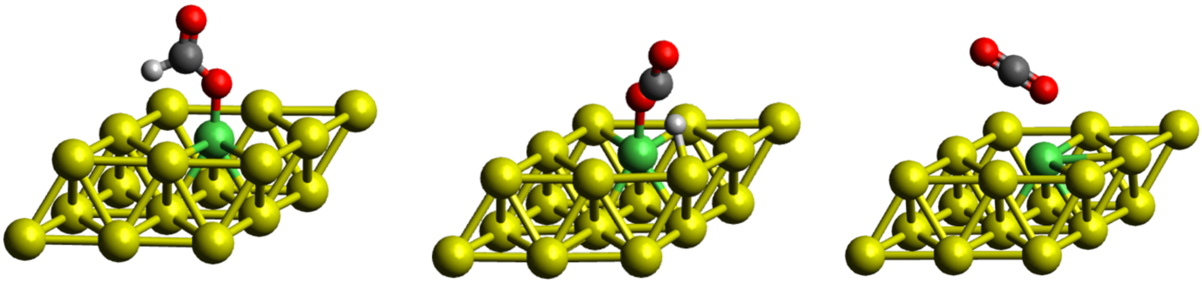

HCOO$_M$ TS CH CO$_2$

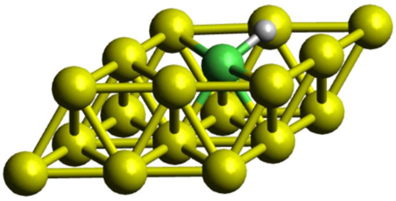

H

Figure S2. Images of molecules, intermediates and transition states configurations for HCOOH decomposition *via* HCOO at Au-Ni surface. The balls represent atoms: Au – yellow, Ni – green, O – red, C – grey, H – white.

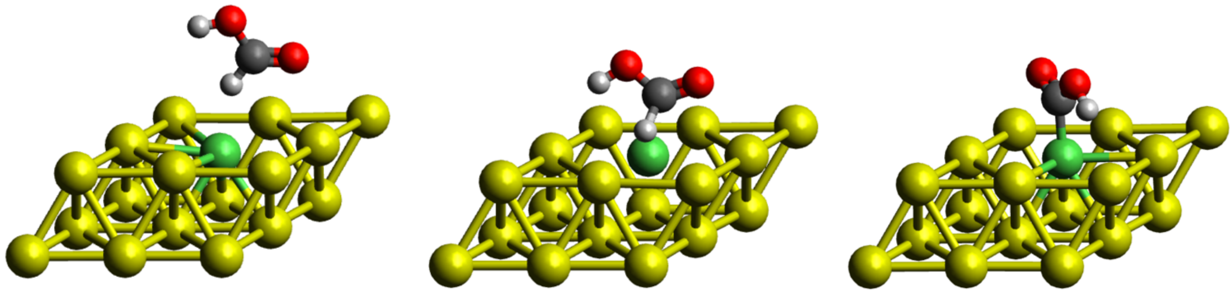

HCOOH TS CH COOH

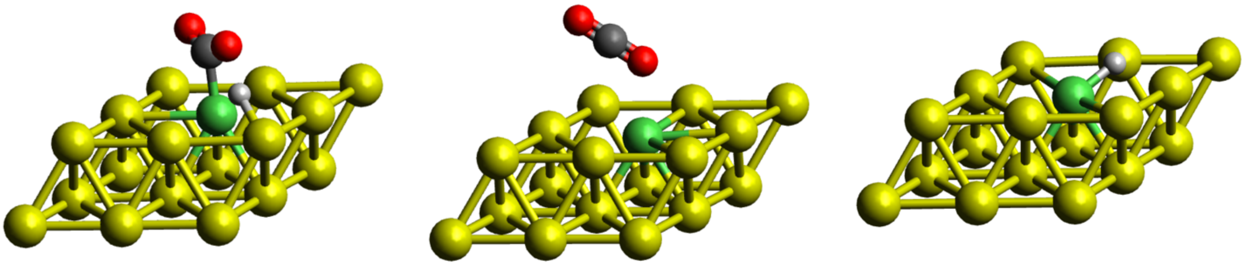

TS OH CO_2 H

Figure S3. Images of molecules, intermediates and transition states configurations for HCOOH decomposition *via* COOH at Au-Ni surface. The balls represents atoms: Au – yellow, Ni – green, O – red, C – grey, H – white.

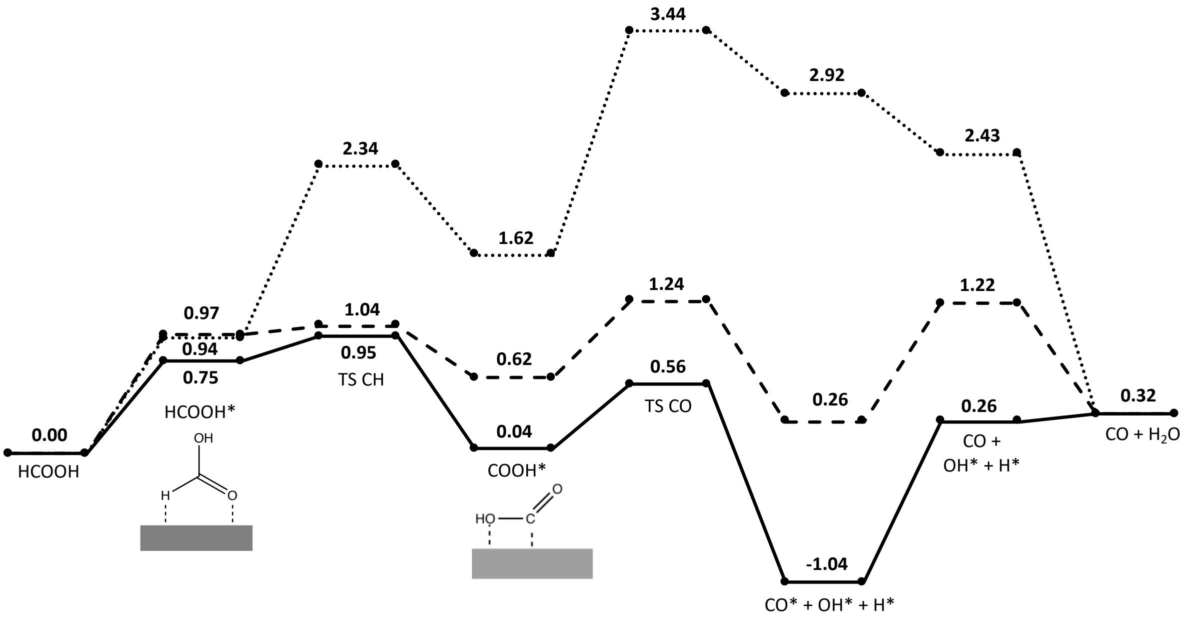

Figure S4. HCOOH dehydration *via* COOH. Gibbs energy profiles for Au (dotted), Ni (plain), Au-Ni bimetallic surfaces (dashed). Gibbs energies given in eV at T=190°C; * means adsorption at the surface.

XPS study

Figure S5 shows the survey spectra for the Au-Ni$_{(Cl)}$/γ-Al$_2$O$_{3(C)}$ catalyst (after in-situ reduction under hydrogen) and the observed elements (C1s for charge effect correction, Ni2p and Au4f for supported phases, Al2p with O1s in inset for the support)

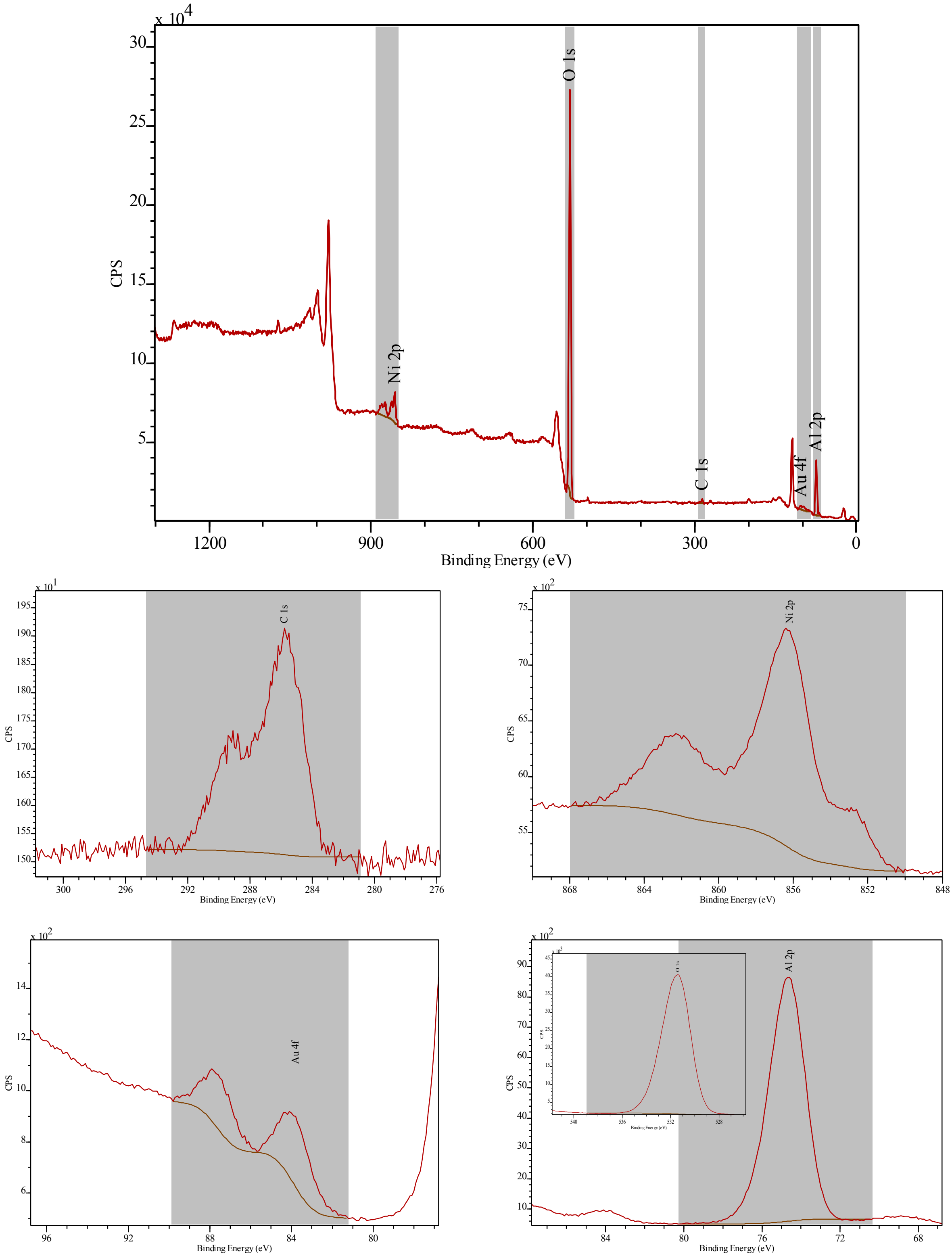

Figure S5 XPS spectra of Au-Ni$_{(Cl)}$/γ-Al$_2$O$_{3(C)}$ catalyst (after in-situ reduction under hydrogen)

TEM Measurements

The identification of the cristal lattice (interplanar spacing d) was done experimentally and compared with the theoretical values for the bulk Au based on JCPDS n° : 03-065-2870 database (Figure S6).

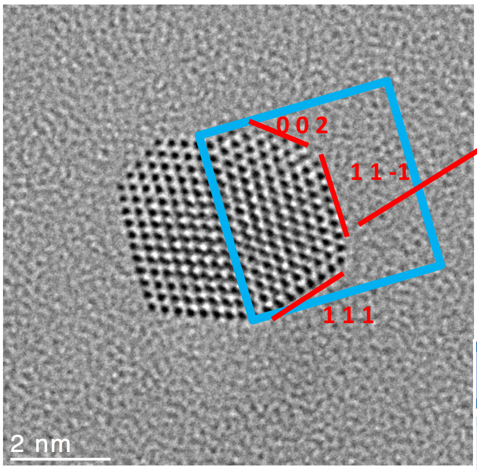

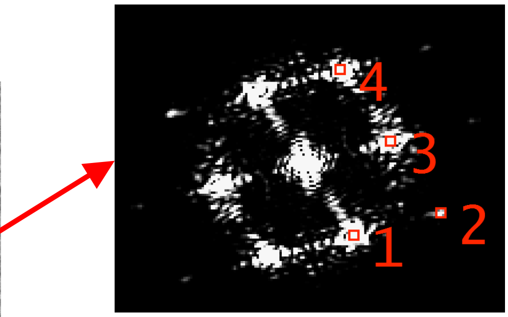

Au
Système : C
S.G : 225
a = 0.40786 nm
JCPDS n° : 03-065-2870

Spot n°	h k l	d (exp.) nm	α (exp.)	d (theo.) nm
1	1 1 1	0.241	0	0.235
2	2 2 0	0.148	35.72	0.144
3	1 1 -1	0.248	71.05	0.235
4	0 0 -2	0.211	126.00	0.204

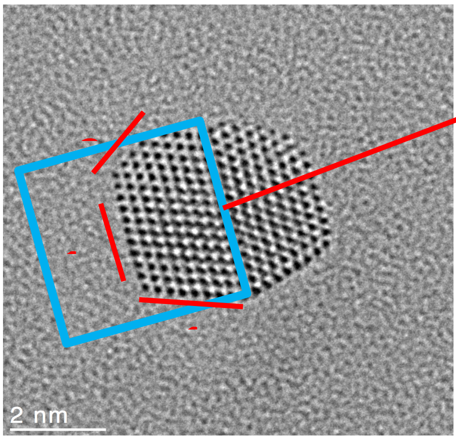

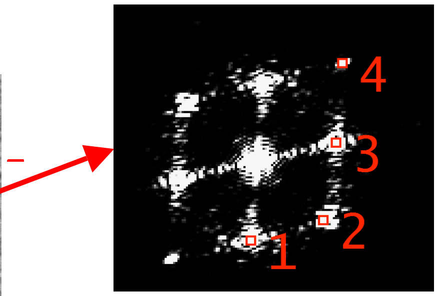

Au
Système : C
S.G : 225
a = 0.40786 nm

Spot n°	h k l	d (exp.) nm	α (exp.)	d (théo.)
1	1 1 -1	0.242	0	0.235
2	2 0 0	0.224	52.03	0.204
3	1 -1 1	0.248	109.75	0.235
4	0 -2 2	0.148	145.26	0.144

Figure S6 The HRTEM images of gold nanoparticle and respective table with the cristal lattice parameters.

Catalytic activity

Selectivity towards gaseous products

By comparing the selectivity to gaseous products for the most active bimetallic catalyst and the monometallic counterparts (table S1), it is possible to observe that the CO/CO_2 ratio is higher in the case of Au/Al_2O_3 than for Au-Ni catalysts, 0.20 vs. 0.18. Those gases were however analysed after the full reaction time (5h), at which a high GVL yield was observed only for bimetallic catalysts and this explains the lowest contribution of hydrogen within the gaseous products. Additionally, the existence of secondary reactions of gaseous products in that case cannot be excluded. When it comes to the monometallic Ni catalyst, the CO/CO_2 ratio is 0.16 This can not be however compared as conversion of formic acid is the lowest (only 53% of FA).

Table S1 Catalytic activity of chosen catalysts together with the selectivity towards gaseous products

Catalyst	FA conversion [%]	LA conversion [%]	GVL yield [%]	Gaseous products [%]			
				H_2	CO	CH_4	CO_2
$Au\text{-}Ni_{(CI)}/\gamma\text{-}Al_2O_{3(C)}$	**100**	**89**	**86**	*16*	*13*	*1*	*70*
$1\%Au/\gamma\text{-}Al_2O_{3(C)}$	**100**	**0**	**0**	*45*	*9*	*1*	*45*
$4\%Ni/\gamma\text{-}Al_2O_{3(C)}$	**53**	**0**	**0**	*37*	*9*	*0*	*54*

Stability of the catalysts

The stability of the catalysts after several catalytic cycles was satisfactory. There was a slight activity drop observed, which could be also related with the smaller amount of the catalysts used for every repetition tests, due to the difficulty of the catalyst recovery after every cycle that led to inevitable catalyst loss with cycles. Moreover, the catalysts were not submitted to any pretreatment between consecutive cycles. This re-usability demonstrates that the potential leaching is contained to a low amount.

Table S 2 Activity of Au-$Ni_{(CI)}$/γ-$Al_2O_{3(C)}$ catalyst after recycling processes in the LA hydrogenation with FA as internal hydrogen source (FALA)

Catalyst	**Recycle step**	**Amount of used catalyst [g]**	**FA conversion [%]**	**LA conversion [%]**	**GVL yield [%]**
AuAu-$Ni_{(CI)}$/γ-$Al_2O_{3(C)}$	1-st	0.60	100	89	86
	2-nd	0.60	100	90	88
	3-rd	0.55	100	80	78
	4-th	0.48	100	73	71
Reaction conditions: 190°C; 2 h; 1 g of LA; 0.4 ml of FA, and autogenic pressure					

ToF –SIMS analysis of catalysts stability after reaction tests

Additionally in order to check the stability of the catalysts (coke formation) after the process we performed the ToF-SIMS study of the catalysts before and after the catalytic cycle Carbon ions were detected on the surface of the analyzed catalysts in almost the same intensity before and after the process (on the range of the mistake). This confirms that no carbon deposit is formed on the surface of the materials during the catalytic test.

Table S3. Normalized intensity of selected ions collected from the surface of the investigated catalysts related to the presence of substances containing carbon.

Normalized intensity of ions	Au-$Ni_{(CI)}$/γ-$Al_2O_{3(C)}$		Au-$Ni_{(DP)}$/γ-$Al_2O_{3(C)}$	
	as prepared	**spent**	**as prepared**	**spent**
C^-	0.023	0.020	0.018	0.021
C_2^-	0.024	0.021	0.021	0.020
$C_2H_5^+$	0.027	0.022	0.025	0.022

---

[1] S. Doniach and M. Sunjic, *J. Phys. C: Solid St. Phys.,* 1970, **3**, 285-291.

[2] D. A. Shirley, *Phys. Rev. B*, 1972, **5**, 4709-4714.